



## CALCULATING HEAVY QUARK DISTRIBUTIONS

John C. Collins

Department of Physics, Illinois Institute of Technology,  
Chicago, Illinois 60616, U.S.A.

and

High Energy Physics Division  
Argonne National Laboratory  
Argonne, Illinois 60439, U.S.A.

Wu-Ki Tung

Department of Physics, Illinois Institute of Technology,  
Chicago, Illinois 60616, U.S.A.

and

Fermi National Accelerator Laboratory  
Batavia, Illinois 60510, U.S.A.

A systematic calculation of the evolution of parton distribution functions including the effects of heavy quark masses is presented. The method involves the use of a special renormalization scheme which ensures ordinary massless evolution with the correct number of active quark flavors at all stages, and specifies appropriate matching conditions at thresholds. This method is applicable to all orders of the perturbation expansion in principle, and it is simple to implement in practice. Results of this calculation using known distributions at low energies as input are examined and compared with published results. The heavy quark distribution functions are found to be about a factor of two larger than the well-known EHLQ results.

### 1. INTRODUCTION

Most interesting high energy processes studied at current accelerators as well as those projected for the future are described in terms of fundamental parton-parton (including gauge boson) interactions. As the consequence of 'factorization theorems',<sup>1</sup> the cross-section for such a process



can typically be written as a sum of convolution integrals, each consisting of a 'hard scattering' cross-section for elementary partons and a product of parton distribution functions for the physical hadrons. Thus reliable determination of the parton distribution functions is a key element in the study of all current and future high energy processes.

Published parameterizations of parton distribution functions are usually determined by fitting some set of data. Typically the data consists of structure functions from deep inelastic lepton scattering, sometimes supplemented by cross-sections for lepton-pair production in hadron-hadron collisions. The fit is made to a set of QCD-motivated parametric functions which approximate the required  $Q^2$ -evolution in some energy range. (Here  $Q$  is the scale of the hard scattering. A typical range of the kinematic variables covered in these fits is  $0.05 < x < 0.8$ ,  $1.5 \text{ GeV} < Q < 15 \text{ GeV}$ ).

Most work on the evolution of parton distribution functions applies the simple Altarelli-Parisi equation with 3 or 4 massless quark flavors, and hence leaves out the direct and indirect effects of the masses of heavy quarks. Parton distribution functions derived this way are clearly suspect for use in the large  $Q$  domain (say of the order of the  $W$ - and  $Z$ -mass and beyond).

Not only are the distributions of the heavy quarks omitted, but the distributions of the light quarks and of the gluon are affected by the neglect of the heavy quarks. The effect is most important in the small  $x$  region, where all the parton distributions (especially the gluon distribution) accumulate at high energies. Reliable values of the parton distribution functions at small  $x$  are, however, precisely what is needed in the calculation of most high energy processes in hadron colliders<sup>2</sup>.

In this paper we describe a concrete calculation of the evolution of parton distributions using the systematic methods of Refs. 3,4,5 to include the effects of heavy quark masses. This method employs a special renormalization scheme whose important property is that all subtractions are done either by minimal subtraction or at zero momentum with massless propagators. It therefore has the distinctive advantage that massless evolution is used at all stages, with matching conditions

at the thresholds. As a result, the rules of calculation of renormalization group coefficients and hard scattering cross-sections are well-defined to all orders, and they are simple to carry out in practice. Herein is the improvement over the theta-function and other methods that have typically been used in other work.<sup>2,6,7</sup>

The calculations are performed by a computer program that was also designed to provide accurate calculations at small values of  $x$ . It carries out the evolution of the parton distributions, given any specified set of parton distribution functions at a chosen initial scale  $Q = Q_0$ , and given a specified value of  $\Lambda_{QCD}$ . We have used the program to calculate the parton distributions obtained by using various starting distributions corresponding to commonly used parameterizations<sup>8</sup>. We compare the results both with each other and with the results of Eichten et al.<sup>2</sup> Above the thresholds, our calculation yields considerably more heavy quarks than the calculation of Eichten et al.

In Sect. 2 we describe the renormalization procedure for crossing a quark flavor threshold. In Sect. 3, we enumerate the QCD parameters which enter the calculation. We discuss in some detail the definition of the running coupling  $\alpha_s(\mu)$  and the relations between various definitions of  $\Lambda_{QCD}$ . Sect. 4 spells out the numerical evolution procedure and Sect. 5 describes the main results of our study. Sect. 6 contains summary remarks and discussion.

## 2. Parton Evolution Across a Mass Threshold

In quantum field theory, parton distribution functions correspond<sup>8</sup> to certain specialized Green's functions. (Alternatively, moments of these functions correspond to hadronic matrix elements of the twist-two operators of the theory.<sup>9</sup>) It follows that the precise definition of these distribution functions must depend on the renormalization scheme adopted. The physical *structure functions* for various experimentally measurable quantities are, of course, renormalization-scheme

independent. They are convolutions of *parton distribution functions* with *hard scattering amplitudes* (corresponding to Wilson coefficients in the language of the operator product expansion). Hence, the hard scattering amplitudes are also renormalization scheme dependent, and this dependence compensates that of the parton distribution functions.

The methods of perturbative QCD are most simply applied either far below mass thresholds (when the decoupling theorem<sup>10</sup> can be invoked) or far above thresholds (when the quarks can be treated as massless). Our methods provide a systematic way of working in threshold regions as well. The methods apply whatever the number of heavy quarks and irrespective of whether their masses are close or far apart. By a heavy quark, we mean one whose renormalized mass parameter is sufficiently larger than  $\Lambda$ . The charmed quark is presumably marginally heavy enough.

For the sake of clarity, let us focus on one single flavor threshold, associated with a quark of mass  $M_{n+1}$ , where  $n$  is the number of quarks with mass less than  $M_{n+1}$ . To define a perturbation expansion in terms of renormalized quantities, we must introduce a scale parameter  $\mu$ . We let  $\alpha_s(\mu)$  be the effective strong coupling at that scale. In a perturbative calculation of a hard-scattering cross-section on an energy scale  $Q$ ,  $\mu$  must be chosen to be of order  $Q$ .

Our parton distributions when calculated at a scale  $\mu$  must reflect the actual physics on scales of order  $\mu$ . In particular, they must reflect the way in which the heavy quark appears. Now, the decoupling theorem tells us that when  $\mu \ll M_{n+1}$ , the effective number of flavors,  $n_{eff}$ , is  $n$ . On the other hand, when  $\mu \gg M_{n+1}$ , we should neglect the mass of the quark, so that  $n_{eff} = n + 1$ : the  $(n + 1)$ th quark participates as fully in a hard scattering on such a scale as the lighter quarks.

Since the value of  $\mu$  does not correspond to exactly one particular value of a momentum, it is not possible to find a precise value of  $\mu$  that corresponds to the quark threshold. Rather we will choose a threshold value  $\mu = \mu_{n+1}$  by the natural *convention* that the effective coupling is continuous. We will see below that in our scheme, with  $\overline{\text{MS}}$  renormalization for light quarks, this threshold value is  $\mu_{n+1} = M_{n+1}$ . Above this value, we define  $n_{eff} = n + 1$ , while below it we define

$$n_{eff} = n.$$

The renormalization scheme we choose to use was first defined by Collins, Wilczek, and Zee.<sup>3,4</sup> It applies the  $\overline{\text{MS}}$  prescription to Feynman diagrams without any heavy quark lines, and zero-momentum subtraction (BPHZ) otherwise. For this purpose, a quark is treated as heavy or light according to whether  $\mu$  is greater or less than the associated threshold, as defined above. Thus if the only relevant heavy quark is the one of mass  $M_{n+1}$ , then the scheme amounts to switching between two schemes,  $R^0$  and  $R^1$ .

The scheme  $R^0$  is exactly the same as the usual  $\overline{\text{MS}}$  scheme: it is an appropriate scheme when  $\mu \gg M_{n+1}$ . The formulas for the coupling  $\alpha_s(\mu)$ , Wilson coefficients and renormalization group coefficients (including the Altarelli-Parisi evolution kernels) are all standard. The number of flavors which appears in these formulas is  $(n+1)$ . These results cannot be extended into the  $\mu \ll M_{n+1}$  region because the perturbation series contain terms such as  $[\alpha_s(\mu) \ln(M_{n+1}/\mu)]^k$ , so that the higher-order terms would not be smaller than the lower-order terms.

In the  $R^1$  scheme, we only apply  $\overline{\text{MS}}$  subtractions to those graphs that have no heavy quark lines. (For the case at hand  $M_{n+1}$  is heavy.) Other graphs are subtracted at zero external momentum, and with the light-quark masses set to zero. It can be demonstrated that this scheme does not induce extra infrared divergences, and that it preserves gauge invariance.<sup>3,4,11</sup> For Green's functions whose external momenta are much less than  $M_{n+1}$ , the  $(n+1)$ th quark flavor is decoupled. This is manifest in this scheme: the effective low-energy theory, with  $n$  quarks, is obtained merely by dropping all graphs that contain heavy quark lines, without needing to adjust the value of the coupling. The formulas for the running coupling  $\alpha_s(\mu)$ , the renormalization group coefficients, the Altarelli-Parisi evolution kernels, etc are the same as in the  $\overline{\text{MS}}$  scheme when the number of flavors is  $n$ . The  $R^1$  scheme is not very useful for Green's functions with momenta far above the threshold, since there are logarithms of the ratio of momenta to the heavy mass.

The overall renormalization scheme, denoted by  $R$ , consists of combining the  $R^0$  scheme above

threshold with the  $R^1$  scheme below threshold. The implementation of this method requires the calculation of the (finite) renormalization coefficients needed for the transition  $R^0 \leftrightarrow R^1$ , and the specification of the threshold where this transition takes place.

Now to first order in  $\alpha_s$ , the relation between the couplings in the two schemes is<sup>5</sup>

$$\alpha_s^1(\mu) = \alpha_s^0(\mu) \left[ 1 - \frac{\alpha_s^0(\mu)}{6\pi} \ln \frac{M_{n+1}^2}{\mu^2} \right]. \quad (1)$$

It is convenient to choose the threshold  $\mu_{n+1}$  such that the transition  $R^0 \leftrightarrow R^1$  results in a continuous effective running coupling

$$\alpha_s(\mu) = \begin{cases} \alpha_s^0(\mu), & \text{when } \mu > \mu_{n+1}, \\ \alpha_s^1(\mu), & \text{when } \mu < \mu_{n+1}. \end{cases} \quad (2)$$

From eq. (1), it is clear that the appropriate choice is

$$\mu_{n+1} = M_{n+1}. \quad (3)$$

The relation between the parton distributions must have the form

$$f_i^1(x, \mu) = f_i^0(x, \mu) + \frac{\alpha_s(\mu)}{2\pi} \int_x^1 \frac{dy}{y} \sum_j C_i^j\left(\frac{x}{y}, \frac{M_{n+1}}{\mu}\right) f_j^0(y, \mu), \quad (4)$$

where  $f_i(x, \mu)$  is the distribution function of parton  $i$  at scale  $\mu$ . The coefficients  $C_i^j$  can be found in Ref. SQ. When  $\mu$  is below  $\mu_{n+1}$ , the distribution function for the  $(n+1)$ th quark is suppressed by a power of its mass, and we therefore neglect it. Thus, the only coefficients  $C_i^j$  in eq. (4) which concern us are  $C_g^g$  and  $C_H^g$ , where  $g$  denotes the gluon and  $H$  the heavy quark. The other coefficients are either higher order in  $\alpha_s$  or else multiply into  $f_H^0$ , which vanishes at threshold. At our chosen threshold,  $\mu_{n+1} = M_{n+1}$ , both  $C_g^g$  and  $C_H^g$  vanish, as they are proportional to  $\ln M_{n+1}/\mu$ , just like the first order term in eq. (1). It follows that all our parton distribution functions are continuous at the threshold given by eq. (3).

### 3. QCD Parameters

The basic QCD parameters are: the total number of quark flavors  $n_f$ , the mass parameters of the quarks,  $M_n$  ( $n = 1, 2, \dots, n_f$ ), and the coupling,  $\alpha_s$ . Now the value of the coupling (and also of the masses) depends on the scale parameter,  $\mu$ , introduced in the renormalization procedure. It is generally convenient to parameterize the dependence on  $\mu$  by a single parameter  $\Lambda$  with the dimensions of mass<sup>12</sup>. Since the value of  $\Lambda$  is scheme dependent and we have chosen a somewhat unusual renormalization scheme, it is necessary to explain our definition of  $\Lambda$ , as well as its relation to the conventional values quoted in the literature.

The parameter  $\Lambda$  enters QCD calculations only through the running coupling  $\alpha_s(\mu)$ . When we have one or more heavy quarks in the theory, the effective number of quark flavors depends on the renormalization scale  $\mu$  (which is usually chosen to be equal to the momentum scale  $Q$  of the application). For  $M_n < \mu < M_{n+1}$ , the effective number of flavors is defined to be  $n$ . Then the effective value of  $\Lambda$  in this region, denoted by  $\Lambda(n)$ , is related to  $\alpha_s(\mu)$  by the second order formula<sup>12</sup>

$$\alpha_s(\mu) = \frac{b_1(n)}{\ln \mu^2 / \Lambda(n)^2} \left( 1 - \frac{b_1(n)^2}{b_2(n)} \frac{\ln \ln \mu^2 / \Lambda(n)^2}{\ln \mu^2 / \Lambda(n)^2} \right), \quad (5)$$

where

$$b_1(n) = \frac{12\pi}{33 - 2n},$$

$$b_2(n) = \frac{24\pi}{153 - 19n}.$$

The values of  $\Lambda(n)$  for different  $n$  are not independent. The relation between adjacent ones,  $\Lambda(n)$  and  $\Lambda(n+1)$ , is determined by the relation (1) between the corresponding couplings. Thus, only one of the  $n_f$  numbers  $\{\Lambda(n)\}$  can be independently chosen. We make the convention that  $\Lambda(n_f)$  is the independent variable and denote it simply by  $\Lambda$ . This is the conventional  $\Lambda_{\overline{\text{MS}}}$  in the complete theory, with  $n_f$  quarks.

Given  $\Lambda (= \Lambda(n_f))$ , we can obtain the values of  $\Lambda(n)$ ,  $n = n_f - 1, n_f - 2, \dots, 1$  numerically, by solving eq. (1) at the threshold. Alternatively, we can expand the two sides of the equation in inverse powers of  $\ln(\mu^2/\Lambda(n+1)^2)$  and take the leadingmost powers. This results in:

$$\begin{aligned} \ln \left[ \frac{\Lambda(n)^2}{\Lambda(n+1)^2} \right] &= \left[ 1 - \frac{b_1(n)}{b_1(n+1)} \right] \ln \left[ \frac{M_{n+1}^2}{\Lambda(n+1)^2} \right] \\ &+ \left[ \frac{b_2(n)}{b_1(n)^2} - \frac{b_2(n+1)}{b_1(n)b_1(n+1)} \right] \ln \ln \left[ \frac{M_{n+1}^2}{\Lambda(n+1)^2} \right] \\ &+ \left[ \frac{b_2(n)}{b_1(n)^2} \right] \ln \left[ \frac{b_1(n+1)}{b_1(n)} \right] + O \left( \frac{1}{\ln(M_{n+1}/\Lambda(n))} \right). \end{aligned} \quad (6)$$

Each time  $\alpha_s(\mu)$  is needed, we first determine  $n$  by the condition  $M_n < \mu < M_{n+1}$ , and then use eq. (5) to evaluate the running coupling (to second order).

A definition of  $\Lambda$  that is often used in phenomenological analyses of data is the "leading order" (or "first-order")  $\Lambda_{LO}$ , which is related to  $\alpha_s(\mu)$  by the first term of eq. (5) with a fixed number of quark flavors  $n$  (usually taken to be 3 or 4).

This definition is simple but incorrect in principle. In particular, from the calculable correction terms, it is known that  $\Lambda_{LO}$  measured in different processes or at different energies will vary in value, although a properly defined  $\Lambda$  should be a constant in QCD. Furthermore, even in work where the full formula eq. (5) is used, the number of quark flavors is often taken to be a constant (typically 4).

It is useful to establish a correspondence between our  $\Lambda$ -parameter and the  $\Lambda$ -parameters used in standard analyses, by requiring approximate equality between the functions  $\alpha_s(\mu)$  in the schemes over a limited range of  $\mu$ . (It is not possible to enforce agreement for all  $\mu$ <sup>12</sup>.) We choose this range to be around  $\mu^2 \sim 10 \text{ GeV}^2$ . Since  $\alpha_s(\mu)$  only varies slowly, the results are not very sensitive to this choice.

In fig. 1 we plot, as functions of our  $\Lambda$ , the equivalent values of  $\Lambda_{LO}$  and of  $\Lambda_{\overline{MS}}$ , with the usual choice  $n = 4$  for these last two values. For our prescription, we have set  $n_f = 6$  and have chosen  $\{M_i, i = 1, \dots, 6\}$  to be equal to their conventional values. (We have assumed  $M_t = 40 \text{ GeV}$ .)



In fig. 2 we plot  $\alpha_s(\mu)$  as a function of  $\mu$  over the range  $1.5 \text{ GeV} < \mu < 10^4 \text{ GeV}$  for the three schemes described above. For the two schemes with fixed flavor number, we have set this number to four. We choose  $\Lambda_{\text{LO}} = 0.2 \text{ GeV}$  and set the  $\Lambda$ -parameters for the other schemes to their corresponding values determined from fig. 1. The graph is divided into two ranges of  $\mu$  in order to show the details of the comparison. Since the function  $\alpha_s(\mu)$  for a fixed number of (massless) quarks has monotonic and *continuous* derivatives, the first-order and  $\overline{\text{MS}}$  curves cross only at one point. On the other hand, our  $\alpha_s(\mu)$  feels the effect of the heavy quark thresholds. The function is required to be continuous at the thresholds; but its first derivative changes its value going through each threshold, reflecting the turning-on of the new flavor degree of freedom. This can be seen in fig. 2 by the fact that our  $\alpha_s(\mu)$  curve oscillates around the first-order  $\alpha_s(\mu)$  curve as we pass the successive thresholds.

It is of obvious interest to compare our results with the widely used parameterization given by EHLQ<sup>2</sup>. So let us note the pertinent features of their procedure for treating heavy quark masses. They choose the threshold,  $\mu_n$  in  $\mu$  for each heavy quark to be *four times* the quark's mass parameter. At the same time  $\alpha_s(\mu)$  is calculated by the lowest order formula and is required to be continuous at  $\mu = \mu_n$ . The consistency of these choices appears to be questionable; however, in practice, the two curves for  $\alpha_s(\mu)$  can be made very close, provided the value of  $\Lambda$  is adjusted appropriately. If we plot  $\alpha_s(\mu)$  based on the EHLQ formula on Figs. 2 a,b, it will interpolate between the first order  $\alpha_s$  (dashed curve) at low  $\mu$  and our full formula (solid line). But the value of  $\Lambda$  that will do this is not the same as any of ours.

#### 4. CALCULATIONS

We apply the renormalization procedure describing in the previous two sections to the renor-

malization group equations obeyed by the parton distribution functions (Altarelli-Parisi equation):<sup>13</sup>

$$\mu \frac{d}{d\mu} f_i^1(x, \mu) = \frac{\alpha_s(\mu)}{2\pi} \int_x^1 \frac{dy}{y} \sum_j P_i^j\left(\frac{x}{y}, \alpha_s(\mu)\right) f_j^0(y, \mu), \quad (7)$$

where  $i, j$  are parton labels, and  $\{P_i^j\}$  are renormalization group coefficients ('evolution' kernel functions). The functions  $\{P_i^j\}$  in our scheme coincide with the standard expressions<sup>14</sup> in the  $\overline{\text{MS}}$  scheme, when the number of quark flavors is set to the effective number of flavors  $n_{eff}$  at the scale  $\mu$ . We solve these integro-differential equations numerically, starting from an initial value  $\mu = Q_{ini}$  and evolving through successive thresholds to obtain the full set of  $\{f_i(x, \mu)\}$  over the desired range of  $x$  and  $\mu$ . At each of the intermediate thresholds, the parton distribution are continuous, for reasons discussed in Sect. 2, but the evolution kernels change due to the opening up of the new quark-flavor channel.

Since existing parton distribution function parameterizations appear to give an adequate representation of experimental deep-inelastic structure functions in the currently available energy range, we do not make any attempt to fit data with our calculations. Our emphasis is on studying the effects of the opening of heavy quark flavor channels on the evolution of parton distribution functions from current energies to those of interest in future accelerators. To this end, we use standard parameterizations of the parton distributions to provide the input set of parton distribution functions at  $\mu = Q_{ini}$ , and then generate the full set of parton distribution functions over the desired range. We then examine the heavy-quark distributions at high energies. We also compare our results with some existing estimates of heavy quark distributions, and compare results obtained with different sets of input with each other.

In solving eq. (7), we first separate the (flavor) singlet and non-singlet parts of the quark distribution functions. Let  $i = 1, 2, \dots, 6$  denote the quark flavors,  $i = -1, \dots, -6$  the corresponding anti-quarks, and  $i = 0$  the gluon. Then we define the singlet-quark distribution function as

$$f^S(x, \mu) = \sum_{i>0} [f_i(x, \mu) + f_{-i}(x, \mu)]. \quad (8)$$

The non-singlet part of each flavor distribution function is then defined as

$$f_i^{NS}(x, \mu) = f_i(x, \mu) - f_S(x, \mu)/2n_{eff}(\mu), \quad (9)$$

where  $n_{eff}(\mu)$  is the number of active quark flavors at scale  $\mu$ .

The singlet quark function  $f^S$  and the gluon function  $f_{i=0}$  satisfy a set of (two) coupled equations. Each of the non-singlet functions  $f_i^{NS}$  evolves independently by itself. Hence, the initial functions  $f_i(x, \mu = Q_{ini})$  are split into singlet and non-singlet pieces according to eqs. (8) and (9); the evolution in  $\mu$  is then performed for  $\{f^S, f_0\}$  and  $\{f_i^{NS}\}$ . Finally we reassemble the results to obtain the full  $f_i(x, \mu)$  for the desired range of  $x$  and  $\mu$ . We do not employ the usual separation of parton distribution functions in terms of ‘valence’ and ‘sea’ distributions. Each of such schemes presumes certain symmetries of the ‘sea’ distributions which are not necessarily a consequence of QCD, and are subject to modifications in the light of improved experimental data.

## 5. RESULTS

Much recent work on high energy processes involving heavy quarks has used the parton distributions calculated by Eichten et al.<sup>2</sup> It is therefore of interest to calculate parton distribution functions in our renormalization scheme using the same input QCD parameters and initial distributions as EHLQ, and to compare the results at high energies.

In general, we obtain heavy quark distribution functions that are substantially larger than the corresponding ones obtained by EHLQ. For a first look, let us check the second moment of the distribution function. It measures the momentum fraction carried by the parton. In fig. 3a we show the second moments of the ‘sea-distributions’ (u, d, s, c, b, and t) from Set 1 of EHLQ as functions of  $Q$  in the range  $2.5 \text{ GeV} < Q < 10^4 \text{ GeV}$ . To compare with these results, we plot in fig. 3b these same moments obtained from our distribution functions computed with the same input distributions at  $Q_{ini} = 2.5 \text{ GeV}$  and equivalent QCD parameters to those of EHLQ.

The moment of the distribution of a heavy quark (c, b, or t), as given by our calculations, evolve at a similar rate in  $\ln Q$  to that for a light quark (u, d, or s), once we are much above the threshold for the heavy quark. On the other hand, the EHLQ moments show two distinct rates of evolution, with the heavy flavors clearly growing more slowly. As a consequence, we obtain substantially more heavy quarks than EHLQ. The ratios of corresponding (heavy quark) moments from the two sets lie in the range 1.6 to 2.0 from  $Q = 10^4$  GeV down to a few times the threshold value for each flavor. The light sea-quark moments behave qualitatively similar for the two sets, with our results somewhat lower than those of EHLQ. The u-, d- and gluon- moments are plotted against  $\ln Q$  for the EHLQ distributions (dashed lines) alongside those from our distributions (solid lines) in fig. 4. We see that the gluon momentum fractions have somewhat different evolution in the intermediate energy range, and that our gluon fraction is smaller (reflecting more ‘leakage’ to heavy quark flavors). The behavior of the u- and d- moments are similar in the two sets, with our results again being slightly smaller than the other set.

The trends indicated by the momentum fraction manifest themselves in other ways. In fig. 5 we present  $\{f_i(x, Q)\}$  as functions of  $\ln Q$  in the same range as above, with  $x$  fixed at  $10^{-3}$ , a typical value of interest at the next generation of accelerators.<sup>2</sup> Fig. 5a shows the sea distributions of EHLQ set 1; and fig. 5b shows the corresponding curves of our calculation. The distinctive slower rate of growth for heavy flavors in the EHLQ set is again apparent. This feature is more pronounced at smaller  $x$ , e.g.  $x = 10^{-4}$ , and less so at higher values of  $x$ . In fig. 6 we plot the distribution functions versus  $x$  in the range  $10^{-4} < x < 5 \times 10^{-2}$  for a fixed value of  $Q = 83$  GeV. Fig. 6a shows the gluon-, u-, and d- curves from EHLQ set 1 and from our work. All three distributions from the two sets behave similarly. Fig. 6b shows the u-, d-, s-, and c- distributions; and fig. 6c the b- and t- distributions. We see that the difference in the size of corresponding heavy quark distributions from the two sets (by about a factor of 2) is relatively uniform in this  $x$  range.

It should be noted that EHLQ adopt mass-dependent evolution kernels, following the prescrip-

tion of Glück, Hoffmann and Reya<sup>15</sup>. The differences produced by the modified kernels are insignificant except near the thresholds. Furthermore, these differences can, in principle, be compensated by differences in the hard-scattering cross-sections, if both schemes are applied self-consistently. The prescription for calculating hard-scattering cross-sections appropriate to matching the prescription for EHLQ's parton distributions has not been explicitly discussed, to our knowledge.

However, we do not believe that the differences in the heavy quark distribution functions between the EHLQ set and ours can be explained by differences in the choice of threshold points and other detailed prescriptions near the thresholds. The reason is that far above the thresholds, the logarithmic derivative of the sea distribution functions and of their moments should be dominated by the gluon term. Thus they should be flavor-independent. This feature is independent of the prescriptions adopted near the thresholds. The logarithmic derivatives can be read off figs. 3-5 simply as the slopes of the curves. It is manifest that our distributions have flavor independent slopes.

We can also investigate the question: How much do our results on the parton distributions, especially for the heavy quarks, depend on the input distributions? The answer can be obtained by comparing results derived from different sets of inputs all of which fit low energy data. In particular, we have systematically compared results derived from input functions of EHLQ set 2 and of the Duke-Owens<sup>16</sup> set 1, in addition to EHLQ set 1 as presented above. The predicted heavy quark momentum fractions are almost the same in all three cases. This is perfectly understandable as heavy quark evolution is driven mostly by the gluon distribution; the gluon momentum fraction is similar in all sets of parton distribution functions.

We show in fig. 7 the momentum fraction carried by the sea distributions,  $u$ ,  $d$ ,  $s$ ,  $c$ ,  $b$ , and  $t$  as functions of  $\ln Q$  in the same range as before. The curves of fig. 7a are calculated using the Duke-Owens parameterization; those of fig. 7b are our results using the Duke-Owens distributions at  $Q = 2.5$  GeV as input. The value of  $\Lambda$  used in the calculation corresponds to that of Duke-

Owens in the sense described in sect. 3. We note that: (i) the  $c$ -,  $b$ -, and  $t$ - curves are almost indistinguishable from the corresponding ones in fig. 3b; (ii) Duke-Owens uses a  $SU(3)$ -symmetric sea, hence the  $u$ -,  $d$ -, and  $s$ -curves coalesce into one; (iii) there are no heavy quark lines in fig. 7a since the Duke-Owens parameterization assumes four (fixed) flavors; and (iv) the abnormal behavior of the two curves in fig. 7a above  $Q \sim 800$  GeV reveals the upper limit of the range of applicability of this parameterization (note the change of scale in the ordinate). For completeness, we show, in fig. 8, the momentum fraction carried by the gluon and the  $u$ - and  $d$ - quarks. Our curves (solid lines), especially the gluon one, are consistently lower than those of Duke-Owens (dashed lines) due to the creation of the heavy quark flavors. In contrast to the second moment, the  $x$ -dependence of the distribution functions for the various flavors and the gluon from the various sets can differ. The difference diminishes, however, as  $Q$  increases.

## 6. DISCUSSION

We have seen that the evolution of parton distribution functions in  $\mu$ , incorporating quark flavor threshold effects, can be formulated in a systematic way utilizing an appropriate renormalization scheme. The scheme adopted here is the natural extension of the conventional  $\overline{MS}$  scheme, giving the appropriate number of active quark flavors for any given scale  $\mu$ . In applying the parton distribution functions calculated in this scheme to physical processes, it is necessary to fold in the relevant hard scattering cross-sections (or Wilson coefficients) defined in the same scheme.

Most phenomenological applications in the literature use the leading order expressions for the hard scattering amplitude and ignore quark masses. This is not a good approximation when large coefficients in the first order QCD correction term are known to exist (e.g.  $\pi^2$ -terms in lepton-pair production), or when the relevant physical variable  $Q$  is not far above some heavy quark threshold. Under the latter circumstance, inclusion of mass effects in the hard scattering amplitude is clearly

needed to properly account for the smooth turning-on of a new threshold for the specific process. Paying attention to both types of correction will ensure a more meaningful comparison of theory with experiments. Failure to do so can lead to misleading discrepancies in fitted values of QCD parameters or in features of the parton distribution functions.

The heavy quark distribution functions in nucleons, derived from our calculations are roughly a factor of 2 bigger than those obtained by EHLQ. More heavy quarks (at small  $x$ ) will enhance processes which are dominated by incoming heavy quarks. A typical case is Higgs production in a mass range where it is made by quark annihilation. (Its coupling to a quark is proportional to the quark's mass.) Even with our distribution functions, however, the heavy quark flavor content of the nucleon is still quite small compared to the values for gluons and valence quarks.

We have seen that the method of generating parton distribution functions by direct numerical solution of the evolution equations works easily for any chosen set of values of input distribution functions and fundamental QCD parameters. They satisfy the QCD renormalization group equations and incorporate heavy flavor thresholds. This method provides a more flexible and more powerful alternative to the use of fixed parameterizations of the parton distributions in a wide variety of applications to high energy processes.

The programs for these calculations are integrated into a package which also contains (a) routines which evaluate the widely used parameterizations for parton distribution functions, and (b) an interactive module which allows the convenient comparison of various parton distribution functions as functions of  $x$  and  $\mu$ , and of moments of parton distribution functions as functions of  $\mu$ . The subprogram to solve the evolution equations contains parameters which control the desired accuracy of the numerical calculations. For any given set of QCD parameters and input functions, the calculation to generate the full set of  $\{f_i(x, \mu = Q)\}$  for  $10^{-4} < x < 1$  and  $2 \text{ GeV} < Q < 10^4 \text{ GeV}$  with less than 2 – 3% error takes a few minutes of CPU time on a VAX 780. (This program is available to interested users upon request.)

## ACKNOWLEDGMENTS

This work was supported in part by the U.S. Department of Energy under contract DE-FG02-85ER-40235 and by the National Science Foundation under grant numbers PHY-82-17352 and PHY-85-07635. JCC would like to thank the Institute for Advanced Study at Princeton for hospitality while part of this work was performed.

## REFERENCES

- [1] D. Amati, R. Petronzio, and G. Veneziano, Nucl. Phys. **B146**, 29 (1978); S.B. Libby and G. Sterman, Phys. Rev. **D18**, 3252 (1978); A.H. Mueller, Phys. Rev. **D18**, 3705 (1978); S. Gupta and A.H. Mueller, Phys. Rev. **D20**, 118 (1979); R.K. Ellis, H. Georgi, M. Machacek, H.D. Politzer and G.G. Ross, Nucl. Phys. **B152**, 285 (1979); J.C. Collins and G. Sterman, Nucl. Phys. **B185**, 172 (1981).
- [2] E. Eichten, I. Hinchliffe, K. Lane and C. Quigg, Rev. Mod. Phys. **56**, 579 (1984).
- [3] J.C. Collins, F. Wilczek and A. Zee, Phys. Rev. **D18**, 242 (1978).
- [4] J.C. Collins, 'Renormalization', (Cambridge University Press, Cambridge, 1984).
- [5] S. Qian, Argonne preprint, ANL-HEP-PR-84-72, and *IIT Thesis* (1985)
- [6] Y. Kazama and Y.P. Yao, Phys. Rev. **D25**, 1605 (1982); W. Wentzel, Nucl. Phys. **B196**, 259 (1982).
- [7] E.g., D.A. Ross, Nucl. Phys. **B140**, 1 (1978).
- [8] J.C. Collins and D.E. Soper, Nucl. Phys. **B194**, 445 (1982).
- [9] D. Gross in 'Methods in Field Theory', R. Balian and J. Zinn-Justin (eds.) (North-Holland, Amsterdam, 1976).
- [10] T. Appelquist and J. Carazzone, Phys. Rev. **D11**, 2856 (1975); K. Symanzik, Commun. Math. Phys. **34**, 7 (1973); E. Witten, Nucl. Phys. **B104**, 445 (1976).
- [11] Kazama and Yao in Ref. 6.
- [12] W. Bardeen et al., Phys. Rev. **D18**, 3098 (1978).
- [13] V.N. Gribov and L.N. Lipatov, Sov. J. Nucl. Phys. **46**, 438, 675 (1972); Yu.L. Dokshitzer, Sov. Phys. JETP **46**, 641 (1977); G. Altarelli, and G. Parisi, Nucl. Phys. **B126**, 298 (1977); P.W. Johnson and W.-K. Tung, Phys. Rev. **D16**, 2769 (1977).
- [14] W. Furmanski and R. Petronzio, Z. Phys. **C11**, 293 (1982).
- [15] M. Glück, E. Hoffmann and E. Reya, Z. Phys. **C13**, 119 (1982).
- [16] D. Duke and J.F. Owens, Phys. Rev. **D30**, 49 (1984).

## FIGURE CAPTIONS

Fig. 1 Equivalent values of  $\Lambda_{\overline{MS}}$  and  $\Lambda_{LO}$  (for 4 massless quark flavors) as functions of  $\Lambda$  (the QCD scale parameter appropriate for 6 flavors with physical mass thresholds). Corresponding  $\Lambda$ 's yield comparable  $\alpha_s(\mu)$  in the range  $2 \text{ GeV} < Q < 5 \text{ GeV}$  when used in their respective contexts.



Fig. 2 The running coupling as a function of  $\mu$  for three definitions of  $\alpha_s(\mu)$  : (i) the solid line represents eq. (5), using 6 quark flavors with decoupling taken into account at lower energies; (ii) the dashed line represents the ‘first order’  $\alpha_s(\mu)$  using 4 flavors; and (iii) the dotted line corresponds to the second order QCD  $\alpha_s(\mu)$  evaluated in the  $\overline{\text{MS}}$  scheme with (fixed) 4 flavors. The  $\Lambda$ -values used are those corresponding to  $\Lambda_{\text{LO}} = 0.2 \text{ GeV}$  (fig. 1). The two parts of the figures shows two separate ranges of  $\mu$ .

Fig. 3 Second moments of the ‘sea distributions’ as functions of  $\ln Q$ . Part (a) is for EHLQ distribution functions; part (b) shows the same moments obtained from our calculation.

Fig. 4 Same as fig. 3 for the valence quarks and gluon. EHLQ results are in dashed lines; our results in solid lines.

Fig. 5 Parton Distribution Functions at fixed  $x = 10^{-3}$  plotted against  $\log Q$ : EHLQ results (dashed lines) in part (a) and our results (solid lines) in part (b).

Fig. 6 Logarithm of Parton Distribution Functions at fixed  $Q = 83 \text{ GeV}$  plotted against  $\log x$ . Keys to the curves are given on the graphs. Part (a) shows the gluon and the valence quarks; part (b) shows the lighter sea-quarks  $u, d, s$ , and  $c$ ; part (c) shows the heavy quarks  $b$  and  $t$ .

Fig. 7 Second moments of sea-quark distributions from Duke-Owens parameterization set 1 (part a) compared with our results (obtained with Duke-Owens input) (part b). Except for the break in the vertical scale in part (a), these plots can be directly compared with fig. 3.

Fig. 8 Same as fig. 7 for the gluon and the valence quarks. (cf., fig. 4).

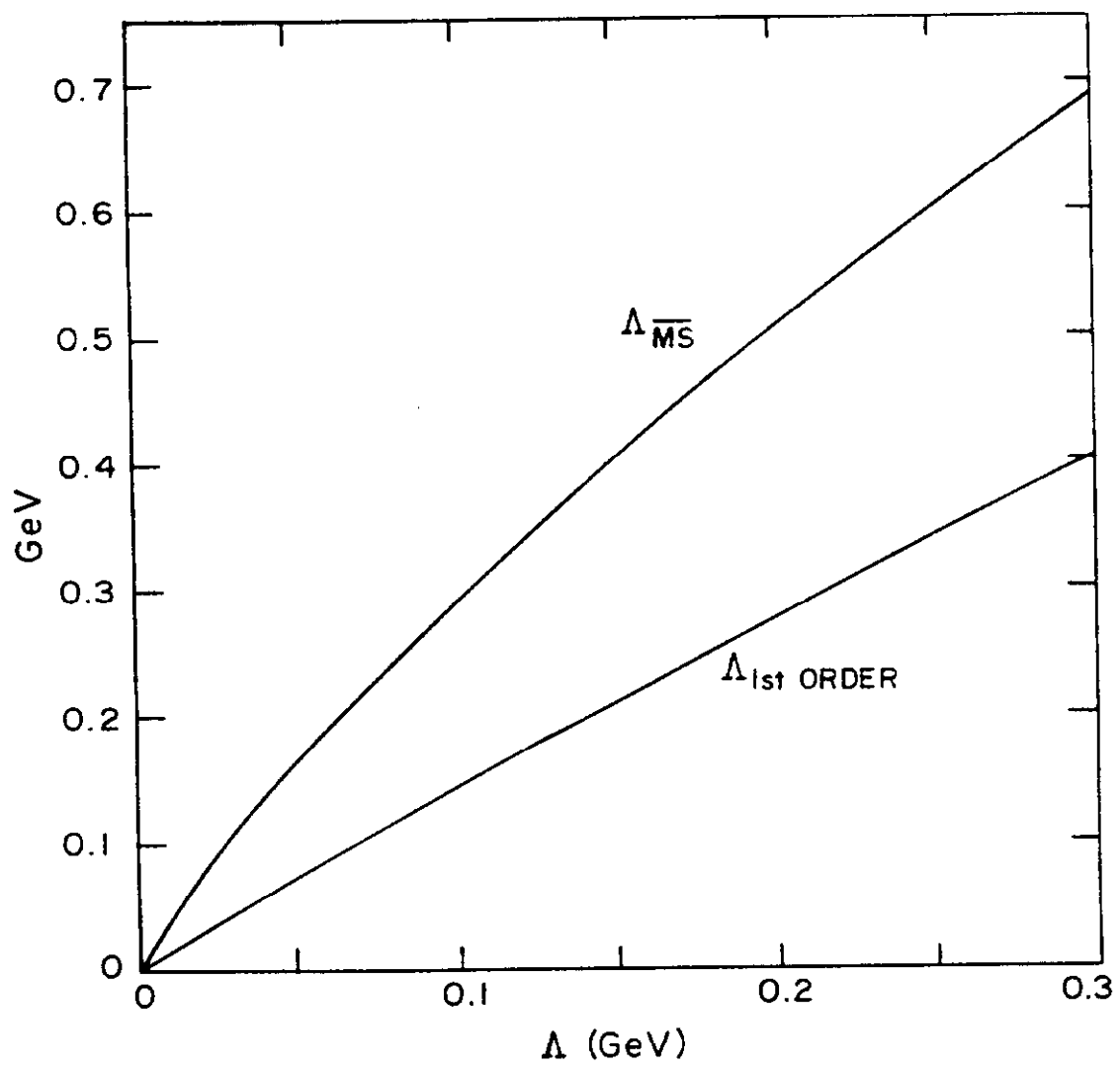


Fig. 1

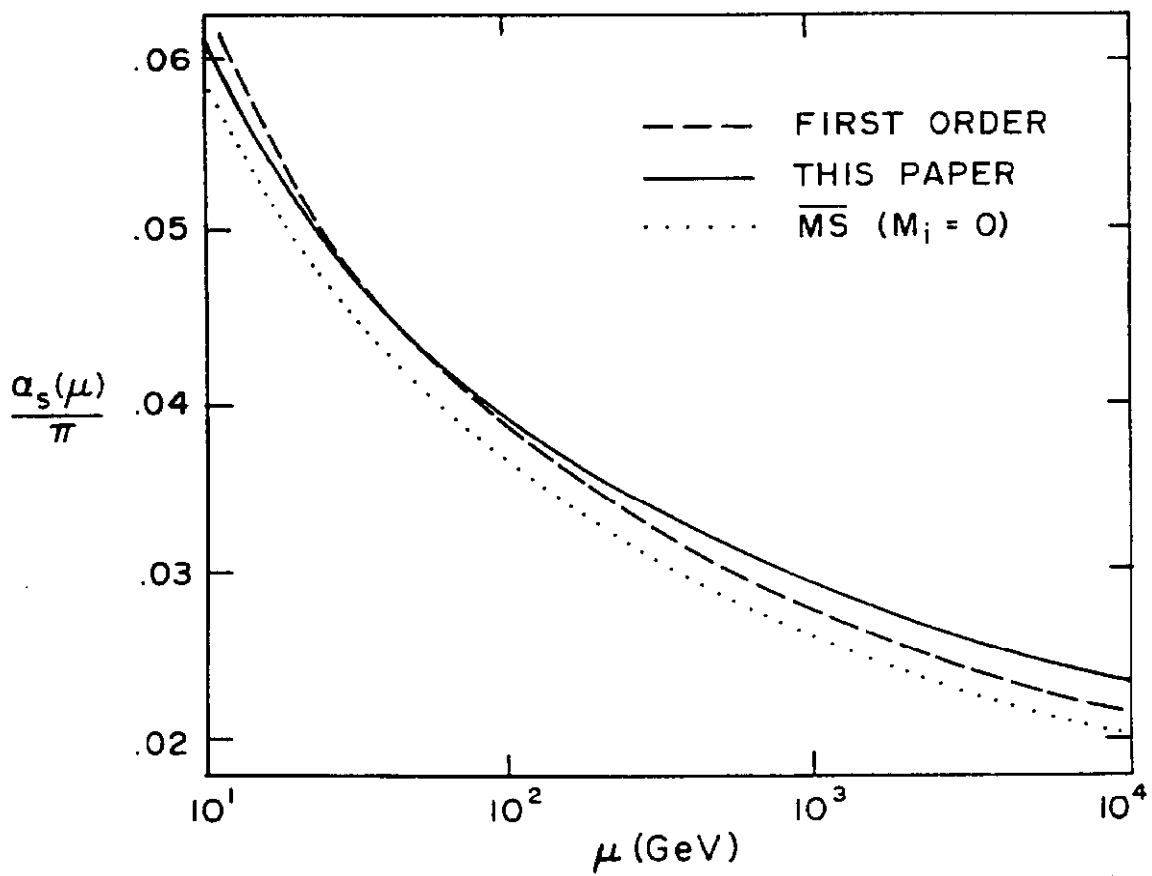
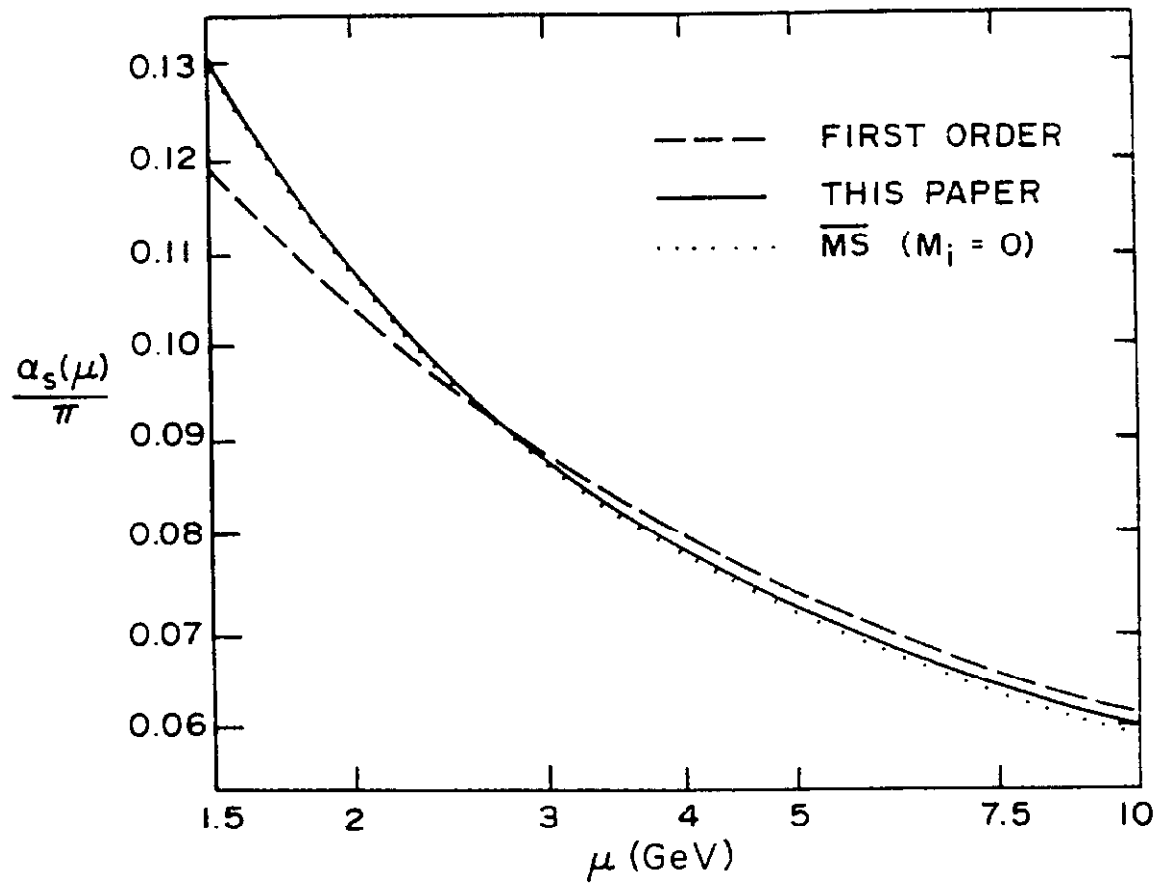


Fig.2

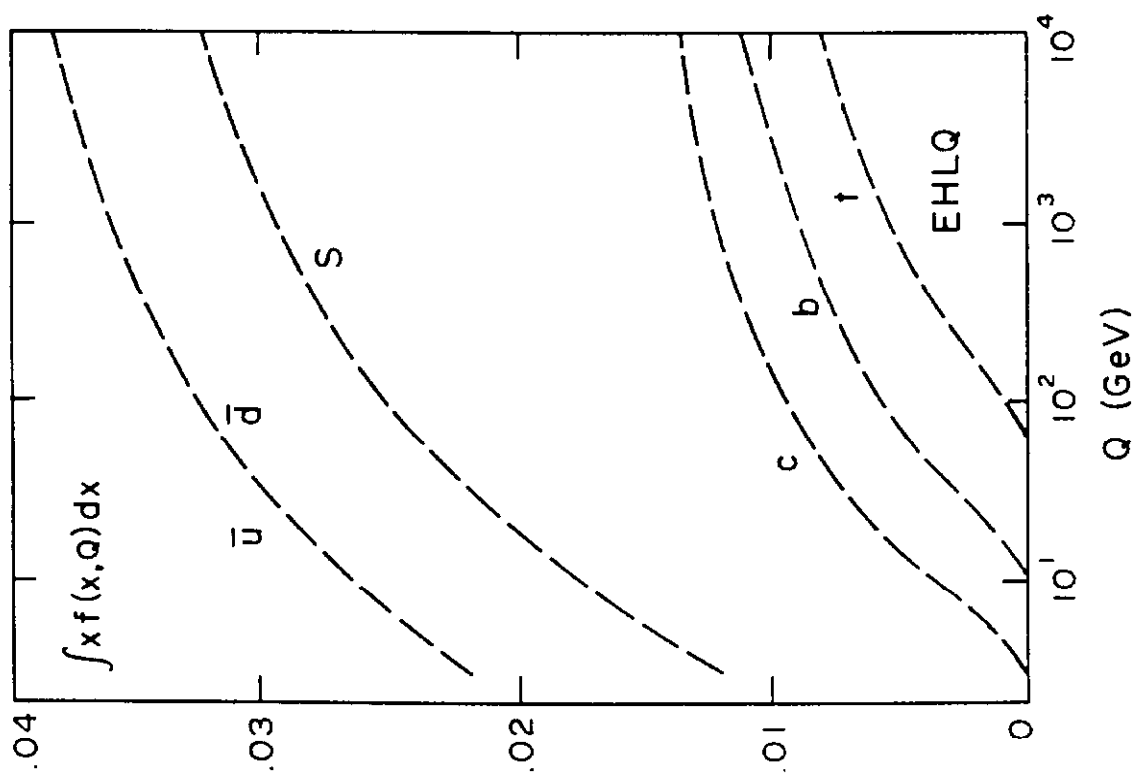
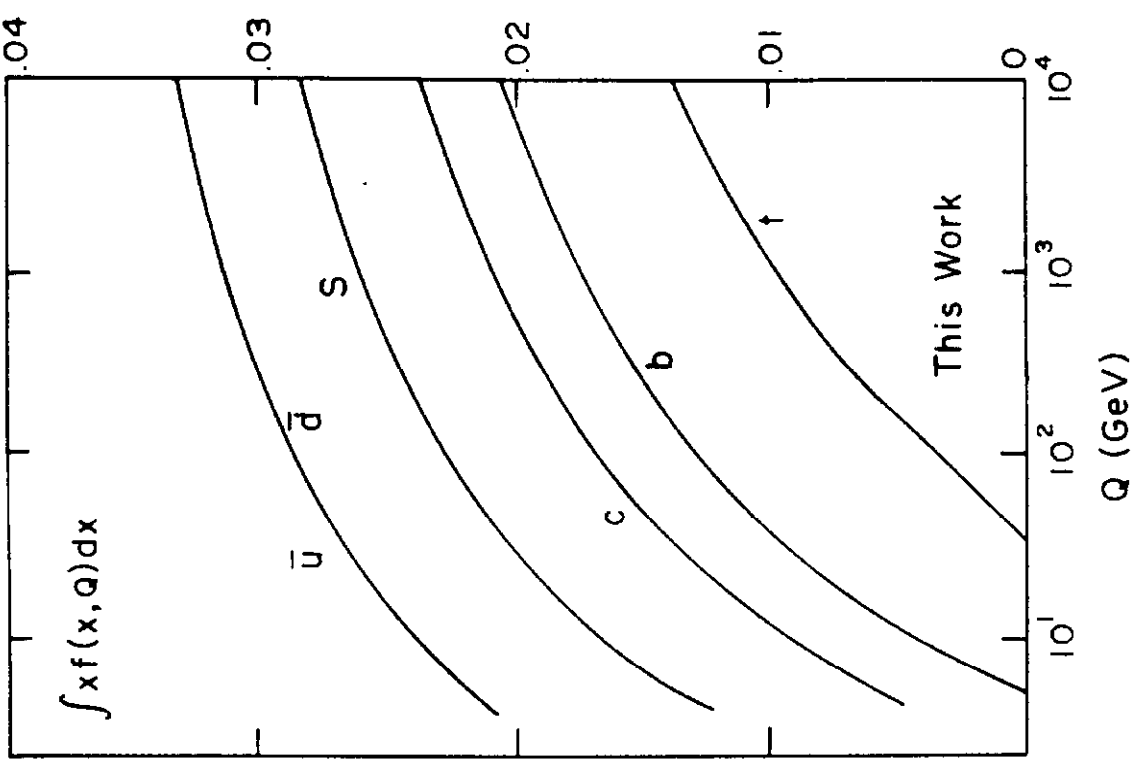


Fig 3

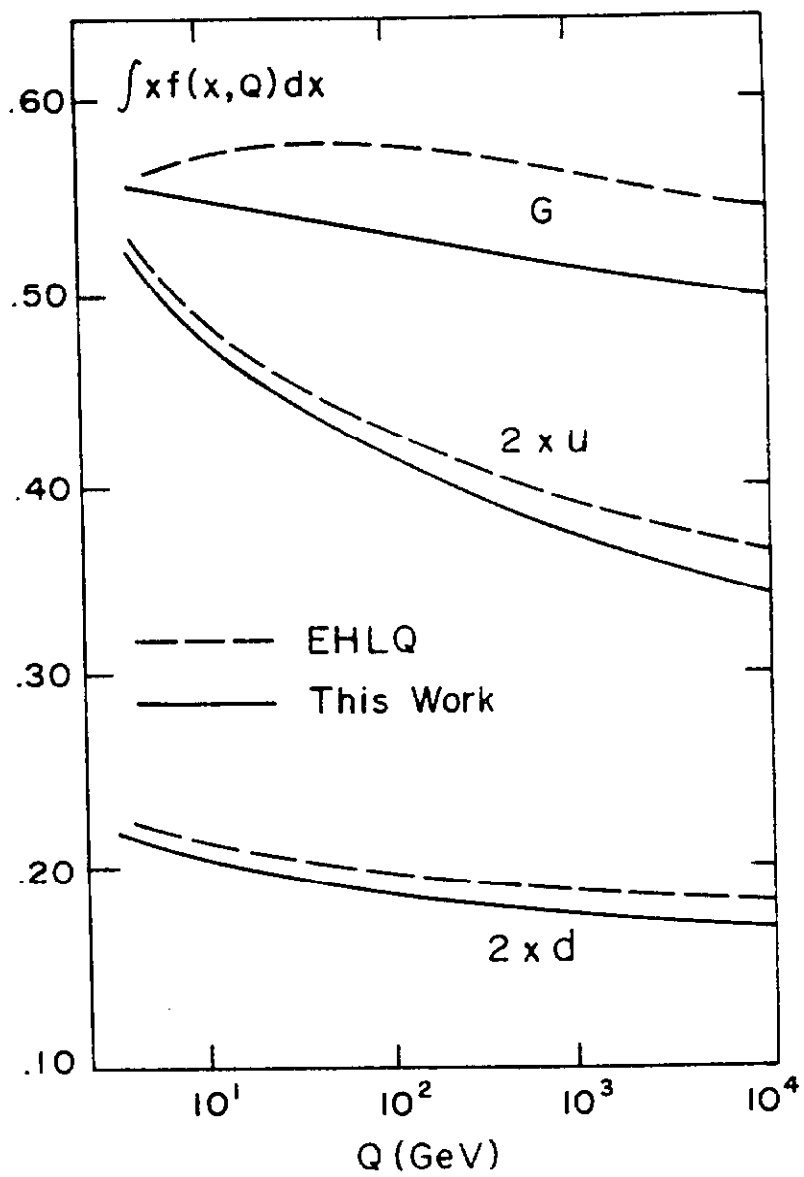


Fig. 4

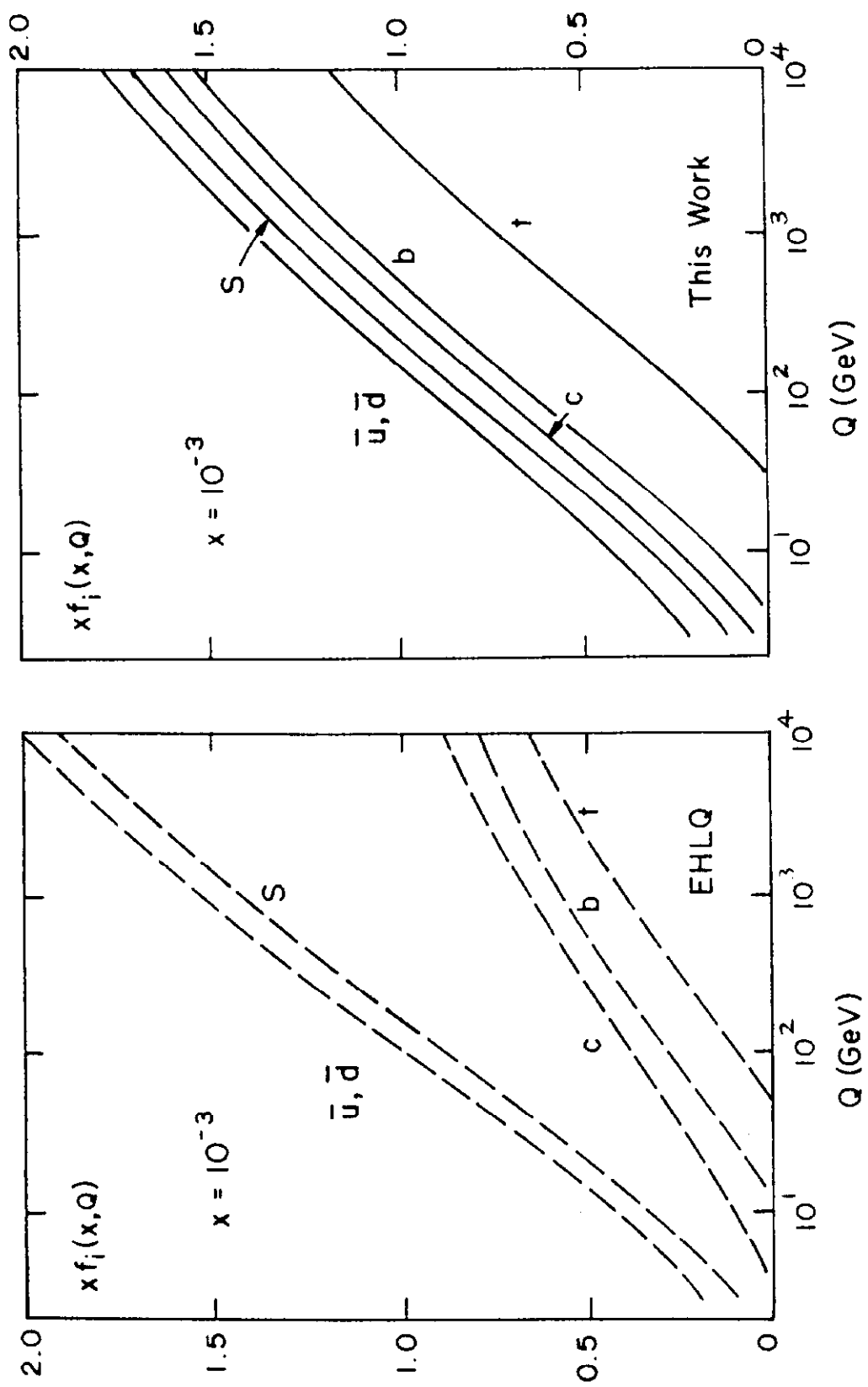


Fig 5

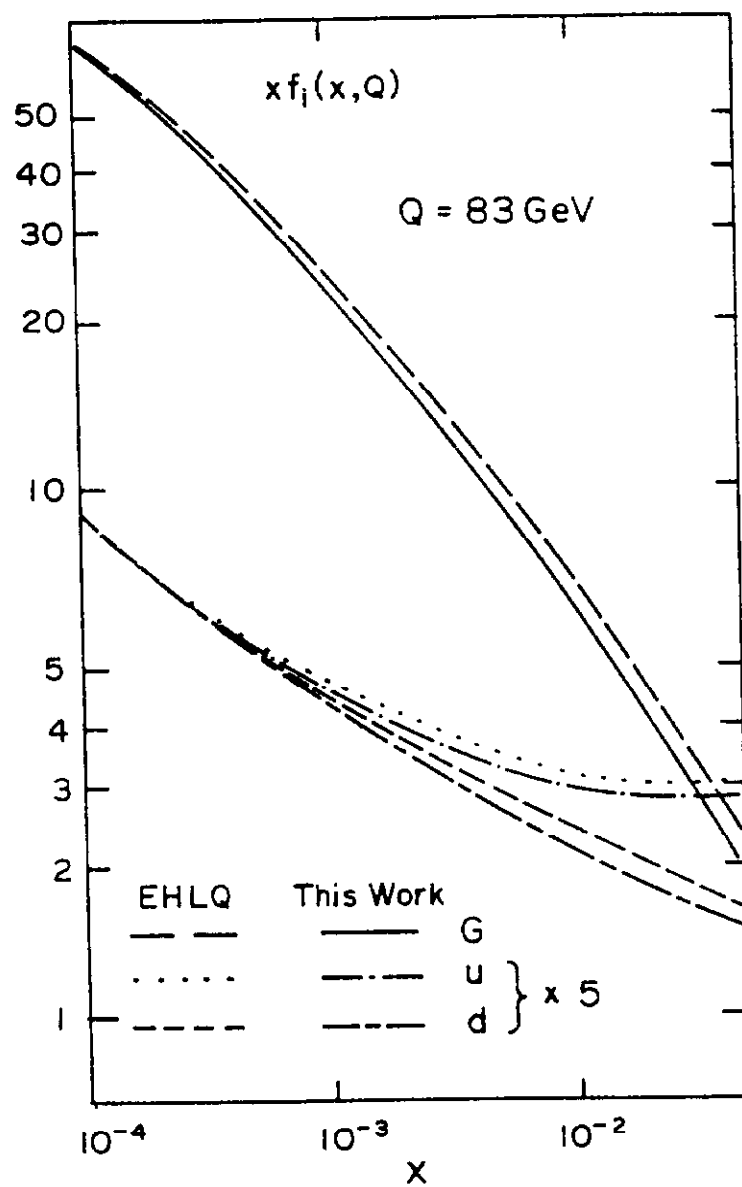


Fig. 6a

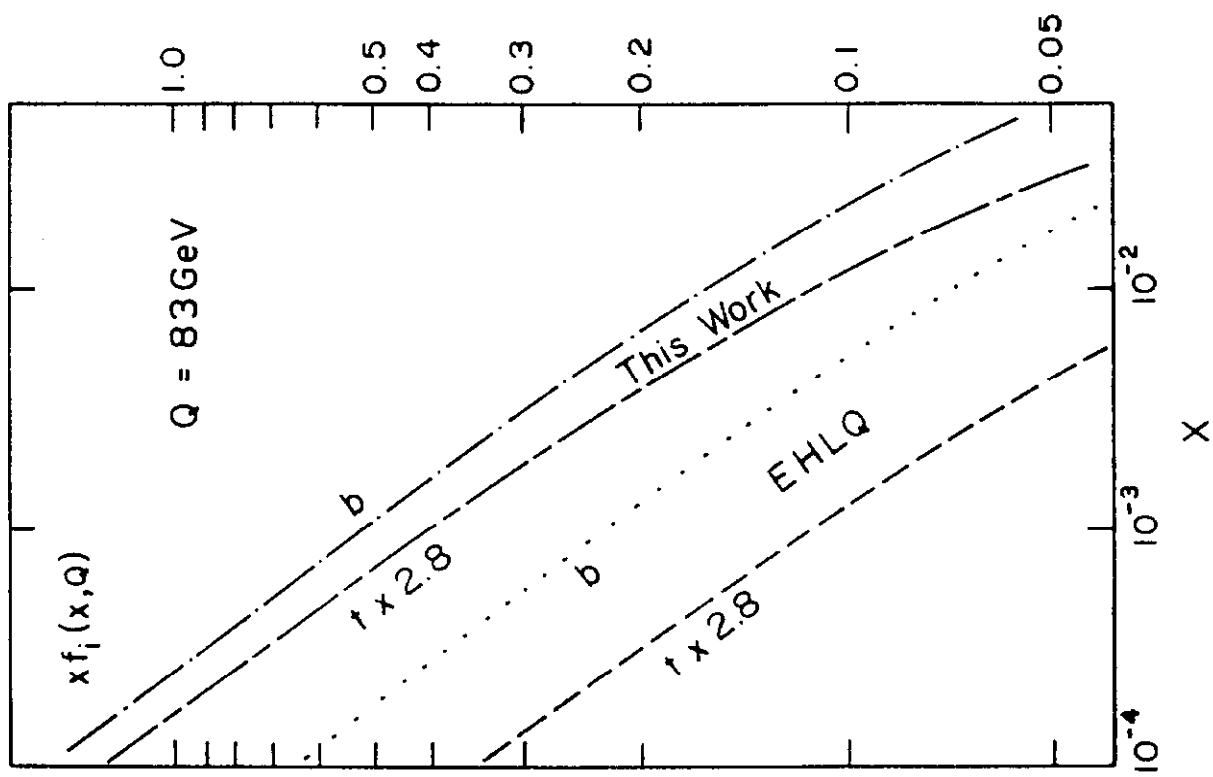


Fig. 6c.

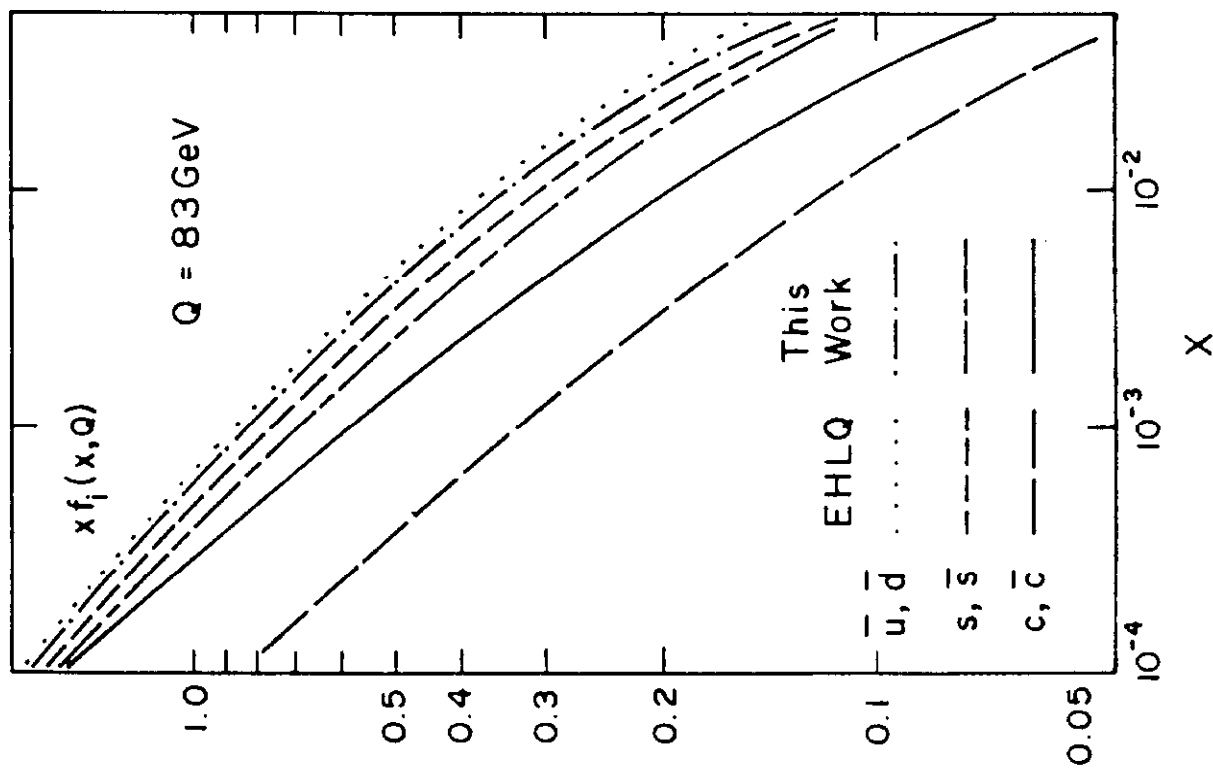


Fig. 6b



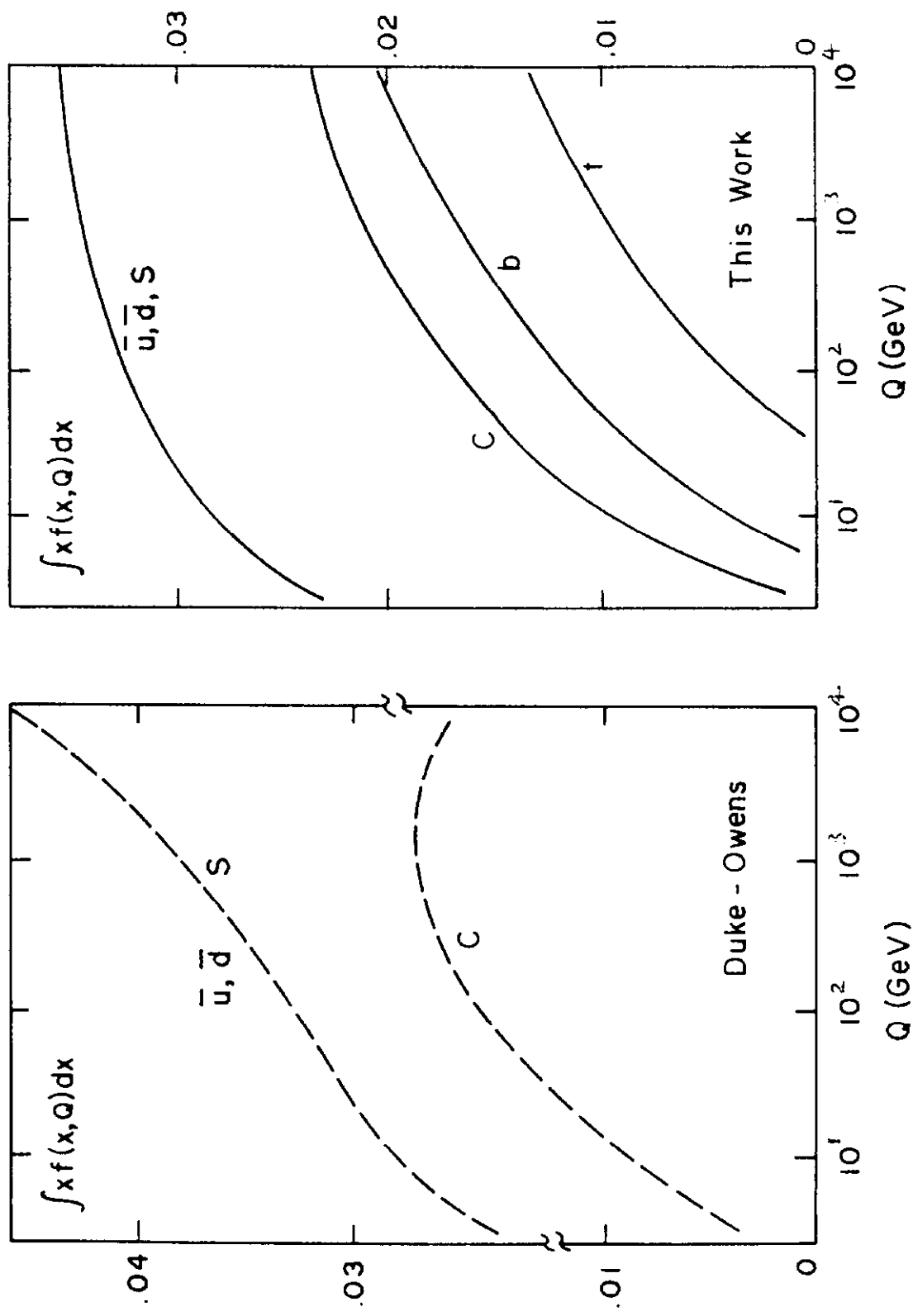


Fig. 7

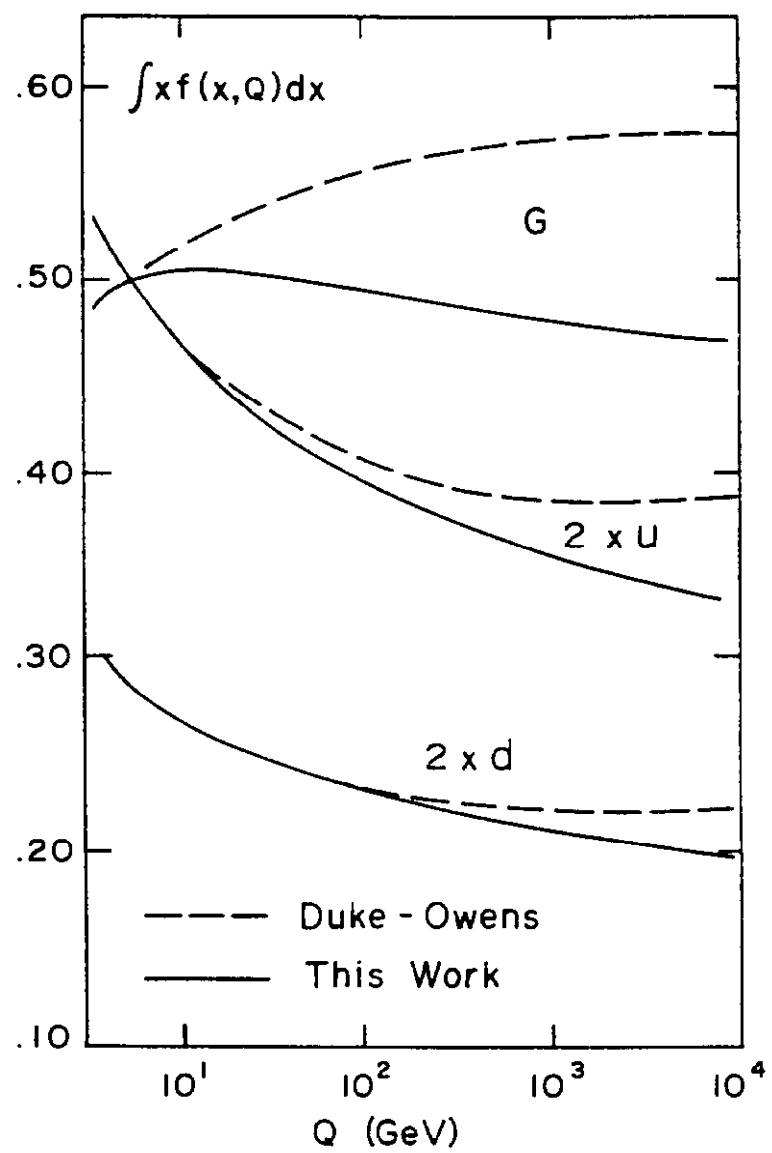


Fig. 8